

Identification and functional characterization of two Δ^{12} -fatty acid desaturases associated with essential linoleic acid biosynthesis in *Physcomitrella patens*

Pichit Chodok · Pradinunt Eiamsa-ard ·
David J. Cove · Ralph S. Quatrano ·
Sireewan Kaewsuwan

Received: 10 January 2013 / Accepted: 7 May 2013 / Published online: 24 May 2013
© Society for Industrial Microbiology and Biotechnology 2013

Abstract Two Δ^{12} -desaturases associated with the primary steps of long-chain polyunsaturated fatty acid (LC-PUFA) biosynthesis were successfully cloned from *Physcomitrella patens* and their functions identified. The open reading frames (ORFs) of PpFAD2-1 and PpFAD2-2 consisted of 1,128 bp and code for 375 amino acids. Their deduced polypeptides showed 62–64 % identity to microsomal Δ^{12} -desaturases from other higher plants, and each contained the three histidine clusters typical of the catalytic domains of such enzymes. Yeast cells transformed with plasmid constructs containing PpFAD2-1 or PpFAD2-2 produced an appreciable amount of hexadecadienoic (16:2 $\Delta^{9,12}$) and linoleic acids (18:2 $\Delta^{9,12}$), not normally present in wild-type yeast cells, indicating that the genes encoded functional Δ^{12} -desaturase enzymes. In addition, reduction of the growth temperature from 30 to 15 °C resulted in increased accumulation of unsaturated fatty acid products.

Keywords *Physcomitrella patens* · Δ^{12} -Fatty acid desaturase · Polyunsaturated fatty acid · *Saccharomyces cerevisiae*

Introduction

Linoleic acid (LA, 18:2 $\Delta^{9,12}$) is an essential fatty acid belonging to the ω -6 polyunsaturated fatty acid group (ω -6 PUFA). LA is required for normal growth of all eukaryotes, as an integral component of cell membranes. Probably more importantly, it is a precursor for synthesis of γ -linolenic acid (GLA, 18:3 $\Delta^{6,9,12}$) and other long-chain PUFAs (LC-PUFAs) in both biosynthetic routes involved in the synthesis of ω -6 and ω -3 polyunsaturated fatty acids by aerobic desaturases and elongase enzymes (Fig. 1) [30]. GLA itself has been claimed to help in prevention and/or treatment of diabetes, eye disease, osteoporosis, premenstrual syndrome, eczema, allergy, high blood pressure, and heart disease [12]. Also, LC-PUFAs such as arachidonic acid (ARA, 20:4 $\Delta^{5,8,11,14}$), eicosapentaenoic acid (EPA, 20:5 $\Delta^{5,8,11,14,17}$), and docosahexaenoic acid (DHA, 22:6 $\Delta^{4,7,10,13,16,19}$) have been widely recognized as having beneficial roles in human health and development. Deficiency of these fatty acids in humans usually results in increased risk of rheumatoid arthritis and inflammation [42], cardiovascular disease [48], neuropsychiatric disorders including dementia and depression [6], and hypertension [45]. Neither DHA nor other PUFAs are produced in sufficient amounts to meet metabolic demands in humans, particularly infants, because mammals in general lack the Δ^{12} - and Δ^{15} -desaturases required for production of these essential fatty acids, LA (18:2 $\Delta^{9,12}$) and α -linolenic acid (ALA, 18:3 $\Delta^{9,12,15}$) [8, 38].

Linoleic acid is normally synthesized by two different pathways that differ in their cellular localization, lipid substrates, and electron donor systems [39]. The microsomal Δ^{12} -fatty acid desaturase (FAD2) is located in the endoplasmic reticulum (ER) and uses phosphatidylcholine (PC) as acyl substrate and nicotinamide adenine

P. Chodok · S. Kaewsuwan (✉)
Marine Natural Products Research Unit, Department of
Pharmacognosy and Pharmaceutical Botany, Faculty of
Pharmaceutical Sciences, Prince of Songkla University,
Songkhla 90112, Thailand
e-mail: songsri.k@psu.ac.th; ksongsri@yahoo.com

P. Eiamsa-ard
Faculty of Science and Technology, Phranakorn si Ayutthaya
Rajabhat University, Phranakorn si Ayutthaya 13000, Thailand

D. J. Cove · R. S. Quatrano
Department of Biology, Washington University in St. Louis,
St. Louis, MO 63130-4899, USA

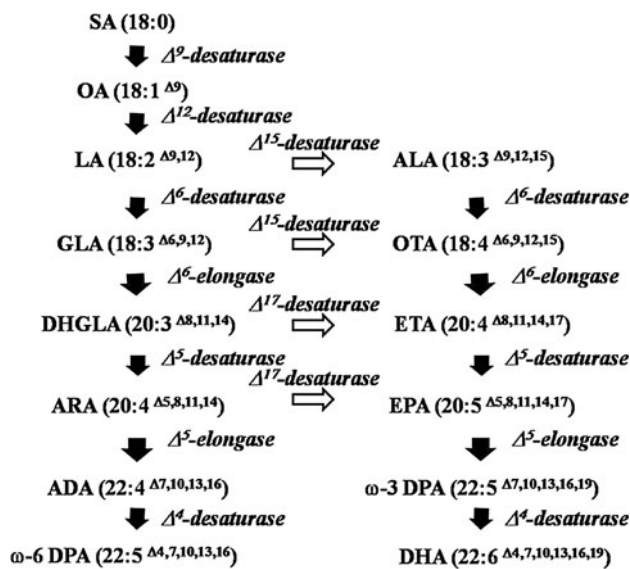


Fig. 1 Biosynthesis pathway of long-chain PUFAs in lower eukaryotes [27]. ADA adrenic acid, ALA α -linolenic acid, ARA arachidonic acid, DHGLA dihomogamma-linolenic acid, DHA docosahexaenoic acid, DPA docosapentaenoic acid, EDA eicosadienoic acid, EPA eicosapentaenoic acid, ETA eicosatetraenoic acid, ETrA eicosatrienoic acid, GLA γ -linolenic acid, LA linoleic acid, OA oleic acid, OTA octadecatetraenoic acid, SA stearic acid

dinucleotide (NADH), NADH-cytochrome b_5 reductase, and cytochrome b_5 as electron donors; this reaction involves concomitant reduction of molecular oxygen to water. In contrast, the plastidial Δ^{12} -fatty acid desaturase (FAD6) is located in the chloroplast and uses primarily glycolipids as acyl carriers and NAD(P)H, ferredoxin-NAD(P) reductase, and ferredoxin as electron donors [22]. Recently, FAD2 genes have been characterized from various organisms including higher plants [10, 18, 21], fungi [29, 49], insects [53], as well as animals [31]. FAD2 and FAD6 appear to be important in chilling sensitivity [27] and salt tolerance [51] of plants, respectively.

The moss *Physcomitrella patens*, a nonseed lower plant, is capable of producing numerous PUFAs, especially high amounts of LA (45.58 mg/l) and ARA (42.89 mg/l) [16]. The ability to synthesize PUFAs makes such lower plants a better target for investigation as a versatile source of PUFAs and also for study of the mechanism of PUFA biosynthesis. To date, five genes involved in PUFA synthesis, encoding Δ^5 - and Δ^6 -desaturases, Δ^6 -elongase, and bifunctional Δ^5/Δ^6 - and trifunctional $\Delta^5/\Delta^6/\Delta^9$ -elongases, have been cloned and characterized from this organism [4, 9, 17, 50], whereas the genes encoding Δ^{12} -desaturase associated with essential LA synthesis have not yet been fully characterized from *P. patens*. Characterization of the biochemistry of these primary desaturation reactions of the LC-PUFA biosynthesis pathway in *P. patens* has therefore attracted a lot of interest to help to understand the

biosynthetic pathways of these important PUFAs that are membrane components and signal precursors.

In the study reported herein, two Δ^{12} -desaturases, PpFAD2-1 and PpFAD2-2, were isolated from *P. patens* and functionally identified by heterologous expression in *Saccharomyces cerevisiae*. The two culture temperatures were investigated to study the effect on the fatty acid accumulation facilitated by these two enzymes.

Materials and methods

Enzymes and chemicals

Restriction endonucleases, polymerases, and other DNA-modifying enzymes were obtained from Takara Bio (Shiga, Japan) unless indicated otherwise. All other chemicals used were of reagent grade from Sigma (St. Louis, MO, USA). Fatty acids were from Nu-Check-Prep (Elysian, MN, USA).

Strains and culture conditions

The Gransden strain of *P. patens* [1] supplied by Prof. Ralph S. Quatrano (Washington University, St. Louis, USA) was used throughout these studies. Protonemata (14 days old) were grown in liquid BCD basal medium to which diammonium tartrate was added to 5 mM, and cultured at 25 °C under continuous light provided by fluorescent tubes [19]. The *S. cerevisiae* strain INVSc1 (*MAT α his3- Δ 1 leu2 trp1-289 ura3-52*; Invitrogen, Carlsbad, CA, USA) was used as a recipient strain in transformation experiments and grown at 30 °C in complex medium containing 1 % bacto-yeast extract, 2 % bacto-peptone, and 2 % D-glucose (Clontech, Mountain View, CA, USA). StrataClone SoloPack *Escherichia coli* (Stratagene, La Jolla, CA, USA) was cultured at 37 °C in Luria–Bertani (LB) medium.

Cloning of putative microsomal Δ^{12} -fatty acid desaturase genes from *P. patens*

Approximately 50 mg fresh weight of protonemal tissue from *P. patens* was ground to fine powder under liquid nitrogen using a precooled mortar and pestle. Total RNA was isolated from the powder using the RNeasy Plant Mini Kit (Qiagen, Valencia, CA, USA), then 5 μ g total RNA was reverse-transcribed with SuperScriptTM RT (Invitrogen, Carlsbad, CA, USA) according to the manufacturer's protocol. The sequence information of fatty acid Δ^{12} -desaturases from various plants together with bioinformatic analysis of the *P. patens* genome database (<http://www.cosmoss.org/> and <http://genome.jgi-psf.org/phy>

scomitrella/physcomitrella.info.html) and NCBI sequence tool Primer-BLAST (<http://www.ncbi.nlm.nih.gov/tools/primer-blast/>) were applied to the specific primer design. The primers used for amplification of the Δ^{12} -fatty acid desaturase genes (PpFAD2-1 and PpFAD2-2) were *Hind*III-PpFAD2-1F: 5'-ATAAAGCTTATGGGGAAAGGAGGC-3' and PpFAD2-1R-*Xho*I: 5'-TATCTCGAGTTATCTACTTTGTTCTTGTACC-3'; *Hind*III-PpFAD2-2F: 5'-ATAAAGCTTATGGGGAAAGGAGGTAGAG-3' and PpFAD2-2R-*Xho*I: 5'-TATCTCGAGTCACTGCACCTGGTTG-3', respectively. The restriction sites (underlined) were added to facilitate the construction of expression vectors. Polymerase chain reaction (PCR) was carried out using complementary DNA (cDNA) as a template with TaKaRa Ex TaqTM DNA polymerase (Takara Bio, Shiga, Japan), and the reactions were conducted using a PCR thermal cycler (Takara Bio, Shiga, Japan) with the following program: 1 min at 94 °C, 0.5 min at 56 °C, and 2.5 min at 72 °C for 35 cycles followed by extension for 10 min at 72 °C. The amplification products were purified by gel electrophoresis, directly ligated into the pSC-A-amp/kan cloning vector (Stratagene, La Jolla, CA, USA), and transformed into StrataClone SoloPack *E. coli* competent cells (Stratagene, La Jolla, CA, USA). The nucleotide sequences of the resulting plasmid DNA were determined, and these plasmids were designated as PpFAD2-1 and PpFAD2-2.

Sequence analysis

Nucleotide sequences of the cDNA clones and their deduced amino acid sequence were identified by using the NCBI BLAST program (<http://www.ncbi.nlm.nih.gov/BLAST/>). Prediction of the open reading frame (ORF) and theoretical molecular weight of the deduced polypeptide was determined using the EditSeq program (version 3.88). Multiple amino acid alignments were performed with ClustalW using default parameters. Prediction of the subcellular localization of the deduced amino acids was conducted using PSORT (<http://www.psort.nibb.ac.jp/form.html>). Transmembrane regions were predicted by using TMHMM Server version 2.0 (<http://www.cbs.dtu.dk/services/TMHMM/>). A phylogenetic tree was constructed using the neighbor-joining method and ProtDist algorithm in the PHYLIP package (version 3.63). The significance level of the neighbor-joining analysis was examined by bootstrap testing with 1,000 repeats. The tree was represented by using TreeView (version 6.6) software.

Functional analysis of PpFAD2-1 and PpFAD2-2 in yeast *S. cerevisiae* INVSc1

The ORFs of PpFAD2-1 and PpFAD2-2 cDNAs from the plasmids PpFAD2-1 and PpFAD2-2, respectively, were

cloned next to the galactose-inducible (*GAL1*) promoter of the yeast expression vector pYES2 (Invitrogen, Carlsbad, CA, USA). The entire ORFs of PpFAD2-1 and PpFAD2-2 were released from the plasmids by digestion with *Hind*III/*Xho*I and subsequently ligated into *Hind*III/*Xho*I-digested pYES2 (Invitrogen, Carlsbad, CA, USA). The corresponding recombinant plasmids were determined by restriction mapping and sequencing, which yielded the plasmids pYpFAD2-1 and pYpFAD2-2. Both expression vectors were separately introduced into *S. cerevisiae* INVSc1 (Invitrogen, Carlsbad, CA, USA) by the *S.c.* Easy-CompTM transformation kit (Invitrogen, Carlsbad, CA, USA), and yeast transformants were selected on complete minimal dropout uracil (CM-Ura; Clontech, Mountain View, CA, USA) solid medium, containing 2 % dextrose (w/v). A single colony was further grown in the liquid medium at 15 °C or 30 °C for 48 h in the presence of 2 % (w/v) raffinose, and expression of the transgenes was induced by addition of galactose (2 % w/v) in the presence of 0.4 mM of various fatty acids (Nu-Check-Prep, Elysian, MN, USA) and 0.7 % (w/v) Tergitol Nonidet P-40 (Sigma, St. Louis, MO, USA). Cells were subsequently harvested by centrifugation, washed twice with sterile distilled water, and dried by lyophilization before determination of their fatty acid composition by gas chromatography (GC).

Fatty acid analysis

Total fatty acids extracted from yeast cells were analyzed by GC of their methyl esters. Lipids from yeast cells were transmethylated with 2.5 % sulfuric acid in methanol at 85 °C for 30 min. Fatty acid methyl esters (FAMES) were then extracted into 1 ml heptane, the organic layer evaporated to dryness with a stream of oxygen-free nitrogen gas, and the residue dissolved in 500 μ l heptane before GC [17]. GC analysis of FAMES was conducted using an Agilent 6890N equipped with an HP-INNOWax capillary column (0.25 mm \times 30 m \times 0.25 μ M) and a flame ionization detector with helium as carrier gas. An aliquot (2 μ l) of each sample extract was injected into the GC column using the injector in split mode. The initial column temperature was 185 °C (0.5 min), and this was increased at a rate of 3.5 °C min⁻¹ to 235 °C (14.3 min), and then maintained at 235 °C for 1.0 min. Fatty acids were identified by comparison with the retention times of fatty acid standards (Nu-Check-Prep, Elysian, MN, USA). Quantitation of fatty acids was estimated from the peak areas extrapolated with the calibration curves of known fatty acid standards. The corresponding fatty acids were further verified with the same conditions by gas chromatography–mass spectrometry (GC–MS) using the HP 6890N Series operating at ionization voltage of 70 eV with a scan range of 50–500 Da.

Southern blotting analysis

Genomic DNA was extracted from *P. patens* tissue using the Nucleon™ PhytoPure™ genomic DNA extraction kit (GE Healthcare, Buckinghamshire, England) according to the manufacturer's instructions. One-microgram aliquot of genomic DNA from *P. patens* was digested with *Hind*III, *Eco*RI, *Eco*RV, *Nco*I, *Xba*I, and *Bam*HI, separated by electrophoresis on a 0.6 % (w/v) agarose gel, and then transferred onto a Biodyne B positively charged 0.45 nylon membrane filter (Pall Life Sciences, Ann Arbor, MI, USA). The filters were hybridized with a full-length cDNA fragment probe of the PpFAD2-1 and PpFAD2-2 coding regions labeled with a PCR Dig Probe Synthesis Kit (Roche Applied Science, Mannheim, Germany). Detection was accomplished with a chemiluminescent substrate (CSPD; Roche Applied Science, Mannheim, Germany) and exposure of CL-XPosure film (Thermo Scientific Inc., Rockford, IL, USA).

Results

Cloning of *P. patens* microsomal Δ^{12} -fatty acid desaturases

To identify genes encoding for the microsomal Δ^{12} -fatty acid desaturase enzymes associated with synthesis of essential fatty acid LA and involved in the primary step of LC-PUFA biosynthesis, NCBI database searches of the *P. patens* genome were conducted to search for sequences similar to those reported for other plant microsomal Δ^{12} -fatty acid desaturases. This allowed for selection of the primers used in PCR reactions for amplifying the cDNA obtained from reverse-transcribed messenger RNA (mRNA) from 14-day-old protonemal tissue of *P. patens*. The full lengths of the potential PpFAD2-1 and PpFAD2-2 cDNAs consisted of 1,128 bp from start (ATG) to stop codons (TAA and TGA, respectively) and encoded a polypeptide of 375 amino acid residues with predicted molecular mass of 43.2 kDa. This is smaller than the other front-end *P. patens* Δ^5 - and Δ^6 - desaturases that have sizes of 54.3 and 59.3 kDa, respectively [9, 17].

As shown in Fig. 2, databank searches and alignment of the two deduced amino acid sequences showed that PpFAD2-1 and PpFAD2-2 shared 91 % identity (95 % similarity), with only 35 amino acids being different in the encoded polypeptides. The *P. patens* FAD2 amino acid sequences shared high homology with an *Olea europaea* microsomal oleate desaturase (OeFAD2) (63–64 % identity) [10] and *Helianthus annuus* microsomal Δ^{12} -fatty acid desaturase (HaFAD2) (62–63 % identity) [24]. In contrast, comparison of the amino acid sequences of both the

PpFAD2-1 and PpFAD2-2 polypeptides with an isolated *Arabidopsis thaliana* plastidial oleate desaturase (AtFAD6) homolog demonstrated only 15–18 % identity [5]. This indicated that the PpFAD2-1 and PpFAD2-2 polypeptides might encode for microsomal rather than plastidial Δ^{12} -fatty acid desaturases.

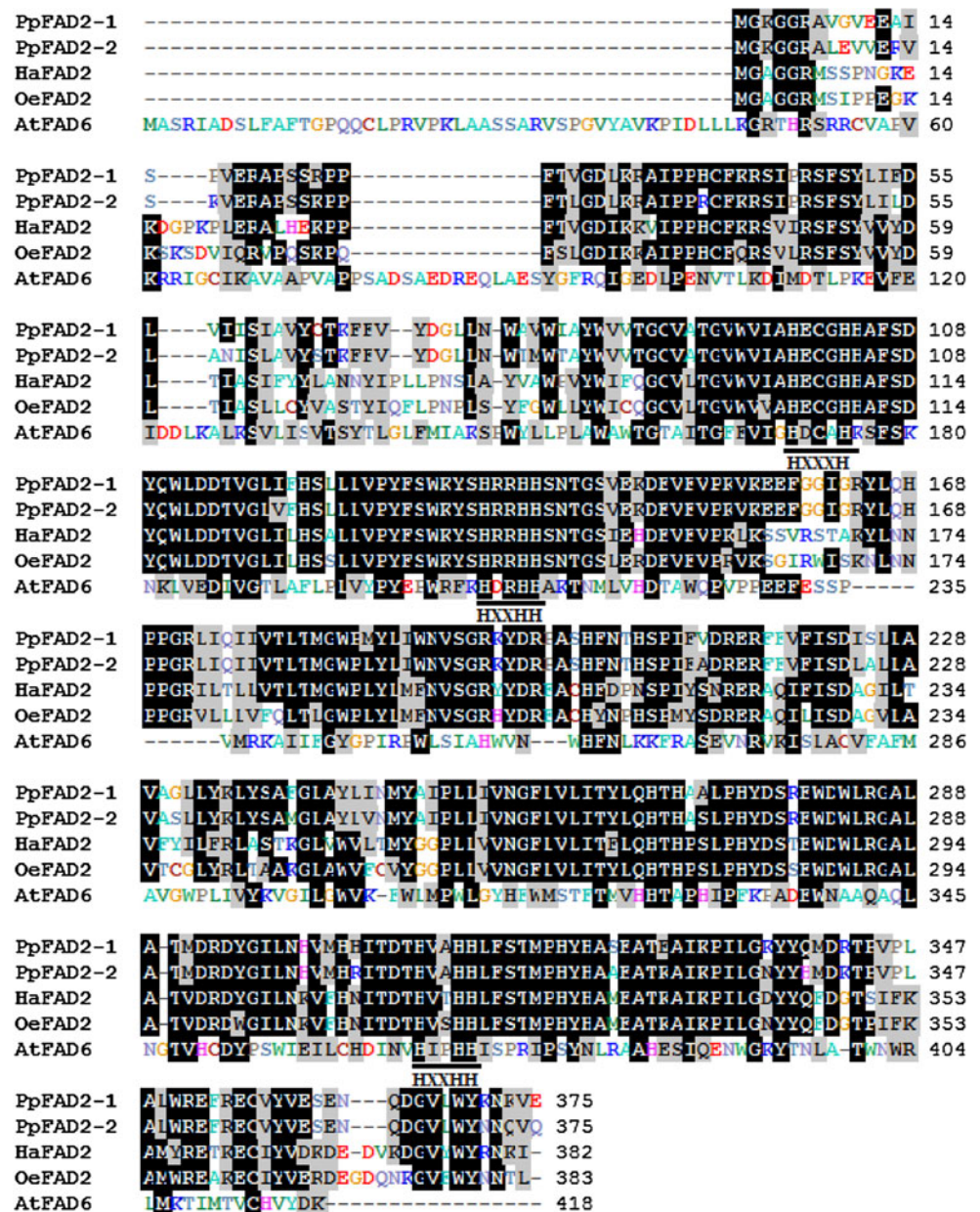
Characterization of putative *P. patens* microsomal Δ^{12} -fatty acid desaturases

Analysis of the deduced amino acid sequence of PpFAD2-1 and PpFAD2-2 revealed the presence of the three conserved histidine-rich motifs: the HXXXXH motif from amino acid residue 99 to 103 (HECGH), the HXXHH motif from amino acid residue 135 to 139 (HRRHH), and the HXXHH motif from amino acid residue 309 to 313 (HVAHH) in the carboxyl terminus (Fig. 2). These conserved motifs are common to all membrane-bound fatty acid desaturases [22, 34, 39]. Eight histidines that are essential elements for desaturase activity [41] were also found in the conserved deduced amino acids of both *P. patens* FAD2 sequences. However, comparison of the amino acid sequences of the histidine boxes of plant microsomal Δ^{12} -fatty acid desaturase (FAD2) and plastidial oleate desaturase (FAD6) indicates that different amino acids are involved. The *P. patens* FAD2-1 and FAD2-2 polypeptides have a HECGH sequence for the first histidine motif that is the same as in other plant FAD2 proteins, while the plant FAD6 desaturases contain an HDCAH sequence. In the second motif, the HRRHH sequence for the FAD2 desaturases is replaced with H(R/D)RHH in the FAD6 desaturase. In addition, the sequence of HVAHH in the third histidine motif found in FAD2 is replaced with HIPHH in the FAD6 desaturases [5].

Hydropathy plots of the PpFAD2-1 and PpFAD2-2 encoded polypeptides contained five and six putative transmembrane domains, respectively (Fig. 3) that correspond to the predicted membrane-spanning domains in other desaturase integral membrane protein models [41]. All of these are short hydrophobic segments and may be single-pass monolayer segments. The three conserved histidine boxes of both PpFAD2-1 and PpFAD2-2 polypeptides were located in the hydrophilic portion.

The phylogenetic relationship of the PpFAD2 polypeptides with various species was constructed based on the alignment of other homologous Δ^{12} -desaturase amino acid sequences (Fig. 4). Generally, plant Δ^{12} -fatty acid desaturases were classified into three major branches: plastidial FAD6 and ER-housekeeping- and seed-type FAD2 [10]. Our results demonstrate that both PpFAD2-1 and PpFAD2-2 cluster with the ER-localized desaturases and form a separate branch within the group of plant FAD2 sequences, implying a lineage more closely associated with higher

Fig. 2 Sequence alignment of deduced amino acids of the *P. patens* microsomal Δ^{12} -fatty acid desaturases (PpFAD2-1 and PpFAD2-2) with other plant Δ^{12} -fatty acid desaturases by ClustalW software. HaFAD2, *Helianthus annuus* microsomal oleate desaturase (GenBank ID: AF251844); OeFAD2, *Olea europaea* microsomal oleate desaturase (GenBank ID: AAW63041); AtFAD6, *Arabidopsis thaliana* plastidial oleate desaturase (GenBank ID: U09503). *Black shades* indicate identical amino acid residues. The three conserved histidine-rich motifs are indicated by *underlines*



plants than lower eukaryotes including algae, fungi, and invertebrates (insects and nematode).

Functional analysis of *P. patens* microsomal Δ^{12} -fatty acid desaturases in *S. cerevisiae*

The functions of the proteins encoded by PpFAD2-1 and PpFAD2-2 were examined by heterologous expression in *S. cerevisiae*. For this aim, the expression constructs, pYpFAD2-1 and pYpFAD2-2, containing the ORFs of PpFAD2-1 and PpFAD2-2, respectively, were separately transformed into *S. cerevisiae* and the fatty acid compositions of the transformants were analyzed by GC. The FAME chromatograms (Fig. 5) of yeast cells transformed with

both plasmids produced two novel fatty acid peaks at retention times (RTs) of 5.3 and 6.8 min. Neither of these is present in wild-type yeast cells. They were identified by comigration and spiking with known authentic fatty acid standards and by the mass spectrometry (MS) fragmentation patterns. The novel fatty acid peak at RT of 5.3 min was identical to hexadecadienoic acid (16:2 $\Delta^{9,12}$), and an additional major peak eluted at RT of 6.8 min was matched to the dienoic fatty acid LA (18:2 $\Delta^{9,12}$) (Fig. 5b, c). These compounds, when investigated by GC-MS, displayed molecular ions of 266 and 294 *m/z*, respectively (Fig. 6a, c), which are the expected molecular ions for methyl esters of hexadecadienoic acid (16:2 $\Delta^{9,12}$) and LA (18:2 $\Delta^{9,12}$), respectively, and the fragmentation patterns were identical

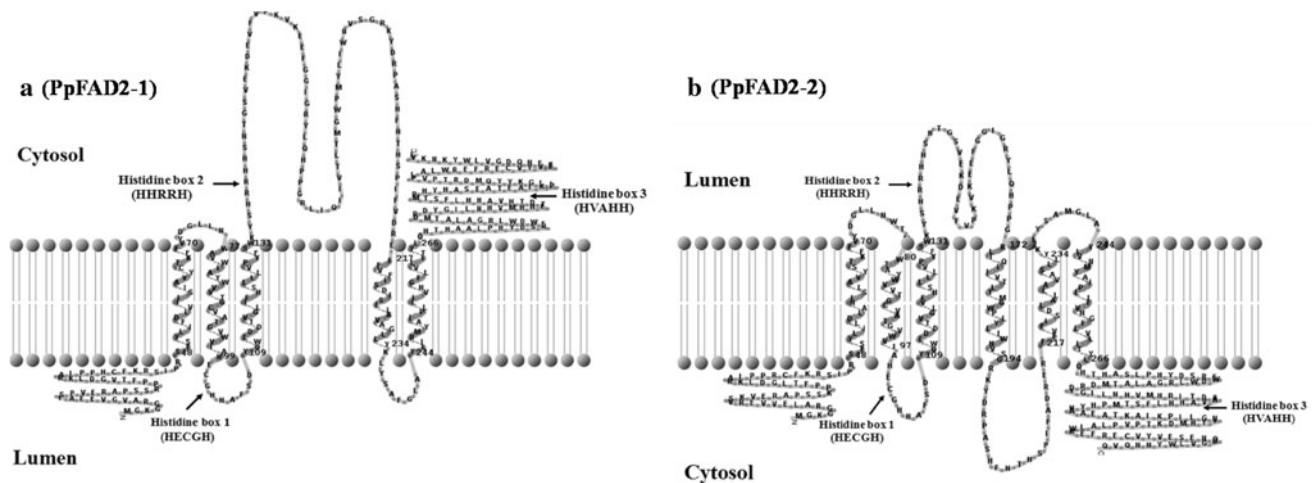


Fig. 3 Transmembrane domains of PpFAD2-1 (a) and PpFAD2-2 (b) predicted by TMHMM Server version 2.0. The three histidine conserved motifs are indicated by *arrows*

to those of the authentic hexadecadienoic acid and LA methyl esters (Fig. 6b, d), respectively. In addition, the amounts of palmitoleic acid (16:1 Δ^9) and oleic acid (OA) (18:1 Δ^9) in the transformed cells were reduced compared with the negative control yeast cells (Fig. 5; Table 1). This clearly demonstrates that PpFAD2-1 and PpFAD2-2 catalyze Δ^{12} -fatty acid desaturation of both endogenous palmitoleic acid (16:1 Δ^9) and OA (18:1 Δ^9) substrates into hexadecadienoic acid (16:2 $\Delta^{9,12}$) and LA (18:2 $\Delta^{9,12}$), respectively.

The accumulation of fatty acids in the transformed yeasts cultivated at 15 and 30 °C is summarized in Table 1. The proportion of LA (18:2 $\Delta^{9,12}$) produced at 15 and 30 °C by the PpFAD2-1 and PpFAD2-2 transformants was 6.4 and 4.5 %, and 3.5 and 3.3 %, respectively, much higher than the level of hexadecadienoic (16:2 $\Delta^{9,12}$) production, which accounted for 2.6 and 1.9 %, and 1.6 and 1.4 %, respectively. These results indicate that PpFAD2-1 and PpFAD2-2 perform Δ^{12} -fatty acid desaturation activity using both C16:1 and C18:1 substrates with a preference for C18:1 over C16:1 fatty acid substrates. PpFAD2-1 has greater Δ^{12} -fatty acid desaturase activity than PpFAD2-2 at both tested culture temperatures. Moreover, the acclimatized condition of low temperature at 15 °C significantly enhanced hexadecadienoic acid (16:2 $\Delta^{9,12}$) and LA (18:2 $\Delta^{9,12}$) facilitated by PpFAD2-1, but not PpFAD2-2.

To investigate whether the *P. patens* microsomal Δ^{12} -fatty acid desaturases were capable of desaturating other exogenous fatty acid substrates, yeast cultures expressing pYpFAD2-1 and pYpFAD2-2 were supplemented with various fatty acids that differ in number and position of their double bond as well as in their chain length (Table 2). All supplied PUFAs were detected from yeast transformants, which confirmed the absorption into the

cells (data not shown), whereas we were unable to detect any product when various di-, tri-, and tetraenoic C₁₈, C₂₀, and C₂₂ fatty acids were fed to yeast cells. From these results we conclude that both PpFAD2-1 and PpFAD2-2 polypeptides appear to be specific only for monoenoic C₁₆ and C₁₈ fatty acids, with 2.9–5.4 and 10.3–18.4 % conversion of palmitoleic acid (16:1 Δ^9) and OA (18:1 Δ^9), respectively, under the culture conditions at 15 and 30 °C (Table 2).

Southern blotting analysis

To investigate the copy numbers of PpFAD2-1 and PpFAD2-2 in the genome of *P. patens*, a Southern blotting experiment was conducted from *P. patens* genomic DNA digested with several noncutting enzymes including *Hind*III, *Eco*RI, *Eco*RV, *Xba*I, and *Bam*HI as well as a single cutting enzyme, *Nco*I, using digoxigenin (DIG)-labeled PpFAD2-1 and PpFAD2-2 probes (Fig. 7). Blotting of the *P. patens* genomic DNA digested with *Hind*III, *Eco*RI, *Eco*RV, *Xba*I, and *Bam*HI and hybridized with the DIG-labeled PpFAD2-1 probe generated a single strongly chemiluminescent fragment (*) of 16.1, 6.3, 8.4, 5.1, and 24.4 kbp, respectively, whereas two expected hybridizing fragments (8.7 and 5.8 kbp) were observed from the *Nco*I digestion (Fig. 7a), which was consistent with the predicted sizes of the relevant fragments from each restriction enzyme digestion. This indicates the presence of a single copy of PpFAD2-1 in the *P. patens* genome. In the same way, hybridization of digested *P. patens* genomic DNA by *Hind*III, *Eco*RI, *Eco*RV, *Xba*I, and *Bam*HI with the DIG-labeled PpFAD2-2 probe detected a single strong signal (***) of 1.2, 4.0, 4.7, 7.5, and 15.4 kbp, respectively, whereas two fragments of the *Nco*I-digested genomic DNA

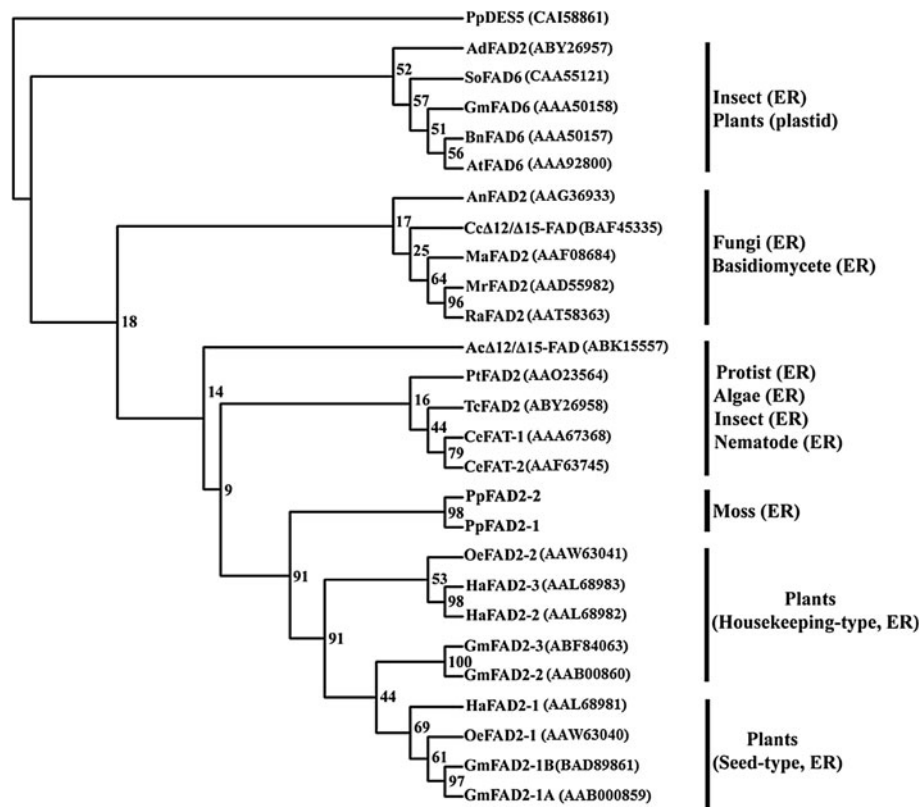


Fig. 4 Phylogenetic tree of Δ^{12} -fatty acid desaturases of PpFAD2-1 and PpFAD2-2 and some other functionally characterized Δ^{12} -fatty acid desaturases. The tree was constructed by the neighbor-joining method using TreeView software. The dendrogram was arbitrarily rooted with the *Physcomitrella patens* Δ^5 -desaturase (PpDES5) sequence (GenBank ID: CAI58861). Positions of the *P. patens* microsomal Δ^{12} -fatty acid desaturase genes are in bold type. The enzymes used for the analysis were: *Acheta domesticus* (AdFAD2, GenBank ID: ABY26957), *Spinacia oleracea* (SoFAD6, GenBank ID: CAA55121), *Glycine max* (GmFAD6, GenBank ID: AAA50158; GmFAD2-1A, GenBank ID: AAB000859; GmFAD2-1B, GenBank ID: BAD89861; GmFAD2-2, GenBank ID: AAB00860; GmFAD2-3, GenBank ID: ABF84063), *Brassica napus* (BnFAD6, GenBank ID: AAA50157), *Arabidopsis thaliana* (AtFAD6, GenBank ID: AAA92800), *Aspergillus nidulans* (AnFAD2, GenBank ID:

AAG36933), *Coprinus cinereus* (Cc Δ^{12}/Δ^{15} -FAD, GenBank ID: BAF45335), *Mortierella alpina* (MaFAD2, GenBank ID: AAF8684), *Mucor rouxii* (MrFAD2, GenBank ID: AAD55982), *Rhizopus arrhizus* (RaFAD2, GenBank ID: AAT58363), *Acanthamoeba castellanii* (Ac Δ^{12}/Δ^{15} -FAD, GenBank ID: ABK15557), *Phaeodactylum tricorutum* (PtFAD2, GenBank ID: AAO23564), *Tribolium castaneum* (TcFAD2, GenBank ID: ABY26958), *Caenorhabditis elegans* (CeFAT-1, GenBank ID: AAA67368; CeFAT-2, GenBank ID: AAF63745), *Physcomitrella patens* (PpFAD2-1, GenBank ID: XP_001757907; PpFAD2-2, XP_001756226), *Olea europaea* (OeFAD2-1, GenBank ID: ABY26957AAW63040; OeFAD2-2, AAW63041), and *Helianthus annuus* (HaFAD2-1, GenBank ID: AAL68981; HaFAD2-2, GenBank ID: AAL68982; HaFAD2-3, GenBank ID: AAL68983). The numbers indicate bootstrap values. ER endoplasmic reticulum

(8.9 and 3.0 kbp) (Fig. 7b) were observed. These results presumably confirmed the sequence difference between PpFAD2-1 and PpFAD2-2 each with a single copy within the *P. patens* genome. However, there are weak bands detected as background signals with each probe, due to the considerable sequence identity (91 %) between PpFAD2-1 and PpFAD2-2.

Discussion

Fatty acids in plants, as in all other organisms, are the major structural components of membrane phospholipids

and triacylglycerol storage oils. Although fatty acid biosynthesis produces saturated fatty acids, in most plant tissues over 75 % of fatty acids are desaturated [28]; Δ^{12} -fatty acid desaturase emerges to be the key enzyme to synthesize LA, a crucial precursor for producing subsequent PUFAs. Likewise, *P. patens* is known to contain high amounts of essential LA (18:2 $\Delta^{9,12}$) [16]. Although several desaturases and elongases have been elucidated from *P. patens* [4, 9, 17, 50], the Δ^{12} -fatty acid desaturase associated with LA biosynthesis has not been functionally identified. In this research, we identified two Δ^{12} -desaturases, PpFAD2-1 and PpFAD2-2, from *P. patens* that share 91 % sequence identity to one another. It was of interest that they exhibited

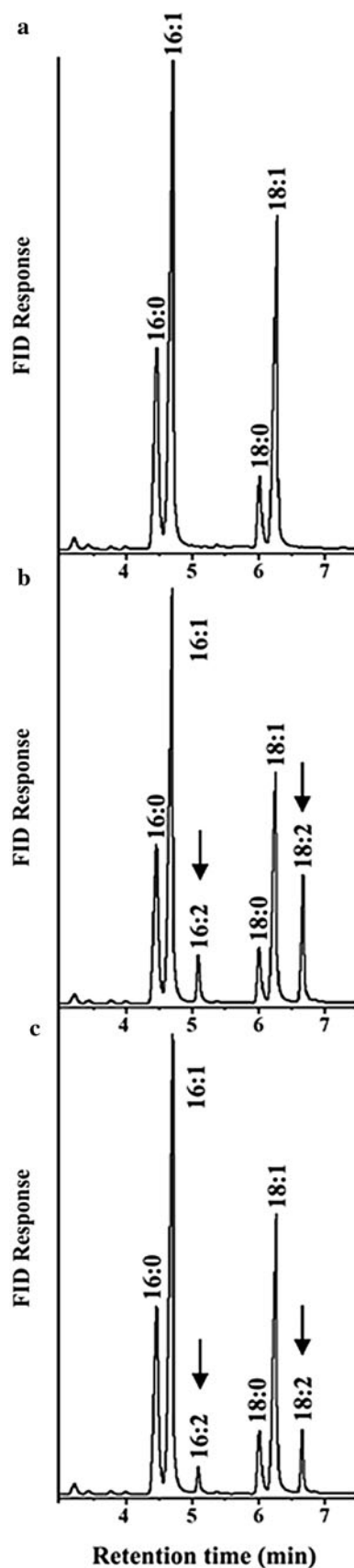


Fig. 5 Identification of hexadecadienoic acid (16:2 $\Delta^{9,12}$) and linoleic acid (18:2 $\Delta^{9,12}$) in transgenic *S. cerevisiae* by GC analysis. The FAMES of total lipid were extracted from yeast transformed with control (empty) pYES2 (a), pYPpFAD2-1 (b), and pYPpFAD2-2 vectors (c) under inducing culture conditions. The endogenous fatty acids found in yeast cell are 16:0, 16:1 Δ^9 , 18:0, and 18:1 Δ^9 . The additional fatty acids corresponding to 16:2 $\Delta^{9,12}$ and 18:2 $\Delta^{9,12}$ are indicated by the arrows

approximately 62–64 % identity to other microsomal Δ^{12} -desaturases of higher plants [10, 24], whereas they had only 15–18 % identity to higher plant plastidyl desaturases [5, 11] or microsomal desaturases of lower eukaryotes (34–41 % identity) [13, 29]. They also had low homology (29–39 % identity) to bifunctional Δ^{12}/Δ^{15} -desaturases from the protozoa *Acanthamoeba castellanii* [37] and the fungus *Coprinus cinereus* [52].

Both PpFAD2s contain three histidine boxes that have similar characteristics to all membrane-bound desaturases, and also were similar to the FAD2s from other plant species. These histidine clusters have been shown to be essential for desaturase activity and act as potential ligands for nonheme iron atoms [39, 41]. Shanklin et al. [40] also reported that a group of different enzymes (desaturases, hydroxylases, and epoxygenases found in animals, fungi, plants, and bacteria that catalyze diverse reactions) also use a reactive center and histidine-rich motifs to form the diiron center of activity where oxygen activation and substrate oxidation occur. Furthermore, the conserved histidine boxes are crucial for desaturase activity, as demonstrated by site-directed mutagenesis studies in the three histidine motifs of the Δ^{12} acyl-lipid desaturase of *Synechocystis*. When only one histidine residue was replaced by an arginine residue, there was complete loss of this enzyme activity [2]. Nevertheless, PpFAD2-1 and PpFAD2-2 did not contain a cytochrome *b*₅-like domain including the HPGG motif in the heme-binding region, as normally present in front-end desaturases. Moreover, the sequence motif HXXHH in the third histidine box started with a histidine (H) instead of a glutamine (Q), which is an obviously conserved feature of methyl-end desaturases including *O. europaea* and *Camelina sativa* Δ^{12} -desaturases [10, 18] as well as a bifunctional *A. castellanii* Δ^{12} -, Δ^{15} -desaturase [37], but is not present in other front-end desaturases such as *P. patens* Δ^5 - and Δ^6 -desaturases [9, 17], *Borago officinalis* and *Nicotiana tabacum* Δ^8 -sphingolipid desaturases [7, 43]. Therefore, the signature sequences for the conserved motifs of microsomal Δ^{12} -fatty acid desaturases should be amended to $[\text{HX}_{(3)}\text{H}]\text{X}_{(30)}[\text{HX}_{(2)}\text{HH}]\text{X}_{(169)}[\text{HX}_{(2)}\text{HH}]$.

From the PSORT algorithm, it was predicted that the PpFAD2-1 and PpFAD2-2 proteins were localized in the ER. The presence of dilysines (K) at the -3 and -5 positions from the C-terminus of PpFAD2-1 also indicated a location

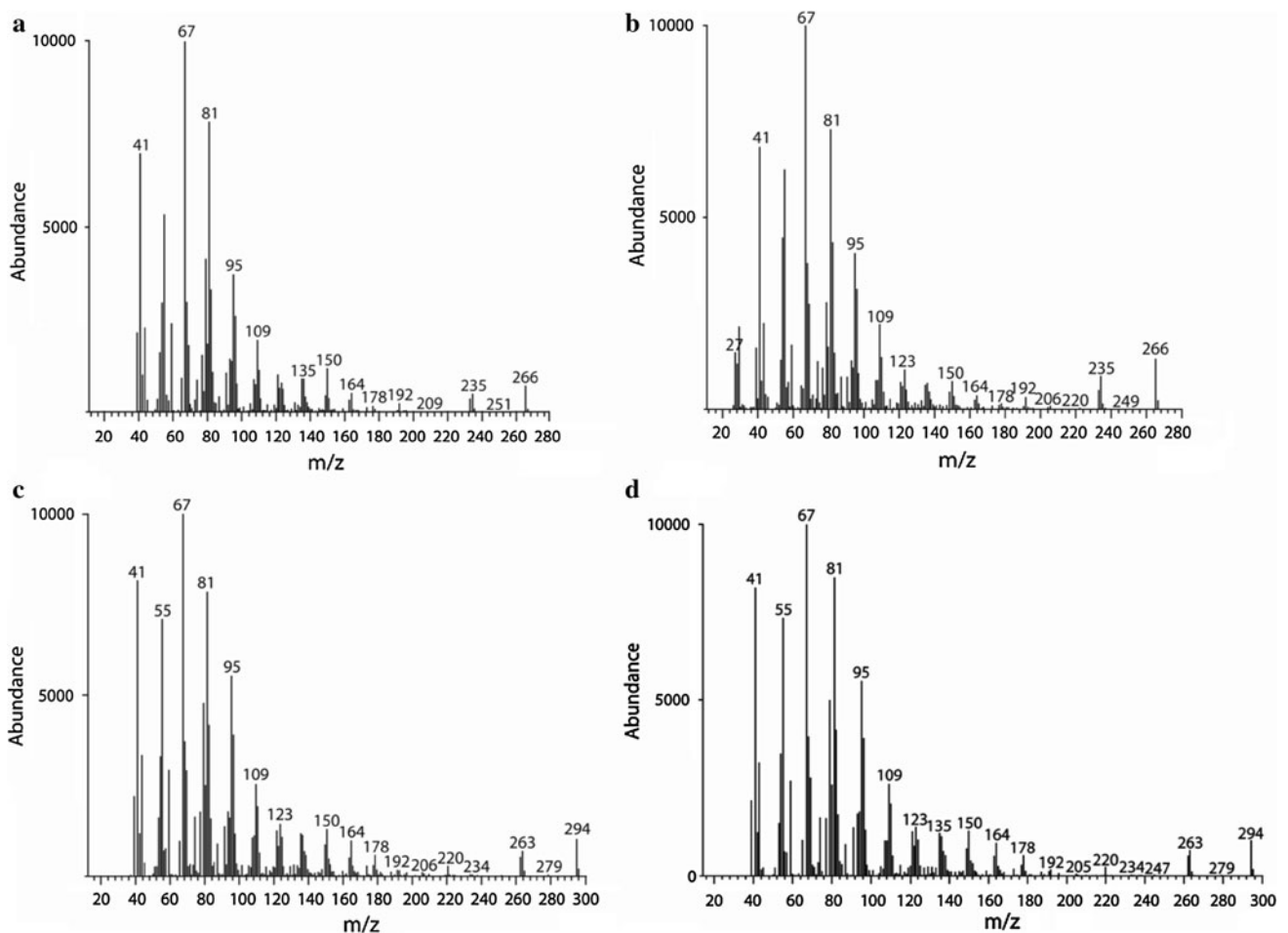


Fig. 6 GC–mass spectrometry analysis of FAMES of the novel peaks identified in yeast carrying pYPpFAD2-1 and pYPpFAD2-2. A comparison is shown of the mass spectra of the novel peak (a, c) and

authentic hexadecadienoic acid (16:2 $\Delta^{9,12}$) and linoleic acid (18:2 $\Delta^{9,12}$) standards (b, d)

Table 1 Fatty acid composition of *S. cerevisiae* INVSc1 cells overexpressing PpFAD2-1 and PpFAD2-2 polypeptides at different temperatures

Plasmid	Temperature (°C)	Fatty acid composition (%) ^a					
		16:0	16:1 (Δ^9)	16:2 ($\Delta^{9,12}$)	18:0	18:1 (Δ^9)	18:2 ($\Delta^{9,12}$)
pYES2	15	20.5 ± 1.5	45.6 ± 1.1	0.0 ± 0.0	5.4 ± 0.3	28.5 ± 1.9	0.0 ± 0.0
	30	20.1 ± 2.1	45.2 ± 1.97	0.0 ± 0.0	6.3 ± 1.0	28.5 ± 1.4	0.0 ± 0.0
pYPpFAD2-1	15	20.2 ± 2.1	41.2 ± 0.5	2.6 ± 0.2	6.1 ± 1.0	23.6 ± 1.1	6.4 ± 1.1
	30	19.8 ± 2.0	41.8 ± 1.5	1.9 ± 0.2 ^b	6.2 ± 0.7	25.8 ± 1.3 ^b	4.5 ± 0.7 ^b
pYPpFAD2-2	15	19.1 ± 0.9	44.5 ± 1.0	1.6 ± 0.2	5.2 ± 0.9	26.1 ± 1.0	3.5 ± 0.5
	30	19.0 ± 1.1	44.2 ± 2.3	1.4 ± 0.1	5.6 ± 0.5	26.5 ± 0.9	3.3 ± 0.4

^a Mean of % total fatty acid based on the three separate experiments

^b Significance compared with 15 °C culture temperature at 95 % confidence level

in the ER [14]. In addition, the predicted PpFAD2-2 polypeptide has a C-terminal aromatic retrieval motif YNNQVQ from amino acid 370 to 375, which is necessary for the maintenance of the FAD2 desaturases in the ER [25]. Therefore, PpFAD2-1 and PpFAD2-2 are most likely

to be microsomal Δ^{12} -desaturases. This observation is also consistent with the FAD2 enzymes being integral membrane, phosphatidylcholine desaturases in the ER.

Heterologous expression of the two PpFAD2 polypeptides in *S. cerevisiae* revealed that neither endogenous

Table 2 Fatty acid substrate specificity of PpFAD2-1 and PpFAD2-2 polypeptides

Fatty acid substrate	Substrate conversion rate at 15 °C (%)			Substrate conversion rate at 30 °C (%)		
	pYES2	pYPPFAD2-1	pYPPFAD2-2	pYES2	pYPPFAD2-1	pYPPFAD2-2
16:1 (Δ^9), palmitoleic acid ^a	nd	5.4 ± 0.2	3.4 ± 0.3	nd	4.0 ± 0.4 ^b	2.9 ± 0.2
18:1 (Δ^9), OA ^a	nd	18.4 ± 0.5	10.8 ± 0.6	nd	13.7 ± 0.4 ^b	10.3 ± 0.3
18:2 ($\Delta^{9,12}$), LA	nd	nd	nd	nd	nd	nd
18:3 ($\Delta^{9,12,15}$), ALA	nd	nd	nd	nd	nd	nd
18:3 ($\Delta^{6,9,12}$), GLA	nd	nd	nd	nd	nd	nd
20:2 ($\Delta^{11,14}$), EDA	nd	nd	nd	nd	nd	nd
20:3 ($\Delta^{11,14,17}$), ETrA	nd	nd	nd	nd	nd	nd
20:3 ($\Delta^{8,11,14}$), DHGLA	nd	nd	nd	nd	nd	nd
20:4 ($\Delta^{5,8,11,14}$), ARA	nd	nd	nd	nd	nd	nd
20:4 ($\Delta^{5,8,11,14,17}$), EPA	nd	nd	nd	nd	nd	nd
22:4 ($\Delta^{7,10,13,16}$), ADA	nd	nd	nd	nd	nd	nd

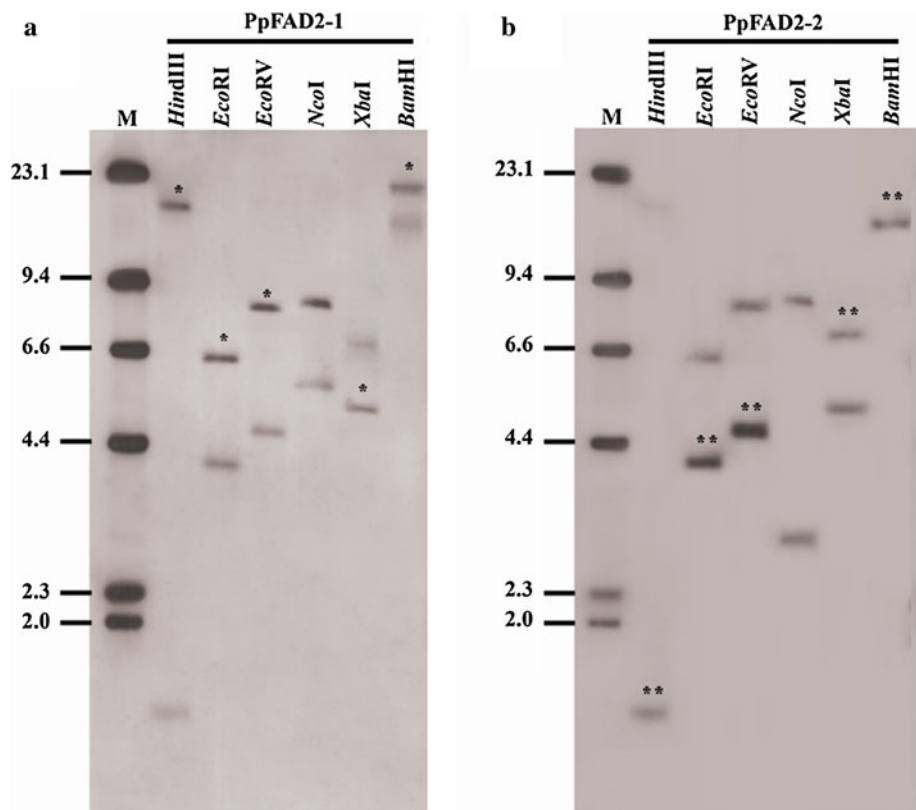
Yeast cells transformed with pYPPFAD2-1 and pYPPFAD2-2 vectors were supplemented with different fatty acids. The FAMES of total lipids under inducing conditions were analyzed by GC, using flame ionization detection. Conversion was calculated as (product × 100)/(substrate + product) using values corresponding to the peak areas of the corresponding signals. Each value is the mean ± standard deviation (SD) from three independent experiments

ADA adrenic acid, ALA α -linolenic acid, ARA arachidonic acid, DHGLA dihomo- γ -linolenic acid, EDA eicosadienoic acid, ETrA eicosatrienoic acid, EPA eicosapentaenoic acid, GLA γ -linolenic acid, LA linoleic acid, nd not detected, OA oleic acid

^a Endogenous fatty acid substrates

^b Significance compared with 15 °C culture temperature at 95 % confidence level

Fig. 7 Southern blotting analysis of *P. patens*. Genomic DNA was digested with *Hind*III, *Eco*RI, *Eco*RV, *Nco*I, *Xba*I, and *Bam*HI and hybridized with PpFAD2-1 (a) and PpFAD2-2 (b) probes. DNA sizes in kbp are indicated on the left. Single and double asterisks indicate the relevant sizes of PpFAD2-1 and PpFAD2-2 detected, respectively



saturated fatty acids, C16:0 and C18:0, nor a variety of exogenous PUFA substrates including LA ($\Delta^{9,12}$), ALA ($\Delta^{9,12,15}$), GLA ($\Delta^{6,9,12}$), EDA (20:2 $\Delta^{11,14}$), ETrA (20:3

$\Delta^{11,14,17}$), DHGLA (20:3 $\Delta^{8,11,14}$), ARA (20:4 $\Delta^{5,8,11,14}$), EPA (20:5 $\Delta^{5,8,11,14,17}$), and ADA (22:4 $\Delta^{7,10,13,16}$) (Table 2) were desaturated by either PpFAD2-1 or

PpFAD2-2. Only two endogenous monoenoic fatty acids, i.e., palmitoleic acid (16:1 Δ^9) and OA (18:1 Δ^9), were converted to hexadecadienoic acid (16:2 $\Delta^{9,12}$) and LA (18:2 $\Delta^{9,12}$), respectively. This evidence confirmed the methyl-end desaturase activity of PpFAD2-1 and PpFAD2-2 cDNAs to be that of microsomal Δ^{12} -fatty acid desaturases with specificity for monoenoic C16 and C18, and a preference for C18:1. Similarly, FAD2s from other higher plants such as *Gossypium hirsutum*, *Tropaeolum majus*, *Glycine max*, *Linum usitatissimum*, and *C. sativa*, the fungal *Caenorhabditis elegans*, and insects such as *Acheta domesticus* and *Tribolium castaneum* have also been shown to have specific activity for C16:1 Δ^9 and C18:1 Δ^9 fatty acid substrates [18, 20, 21, 26, 31, 32, 53]. In contrast, the FAD2s from the filamentous fungus *Rhizopus arrhizus* and the higher plant *O. europaea* were able to convert only 18:1 Δ^9 into 18:2 $\Delta^{9,12}$ [10, 29, 49]. Although the reasons for these variations remain to be elucidated, the diverse hydrophobic profiles of FAD2s that indicate different transmembrane topologies among various organisms may be useful to help clarify this puzzle. However, the amount of C16:2 $\Delta^{9,12}$ and C18:2 $\Delta^{9,12}$ produced in yeast cells by PpFAD2-1 is superior to that by PpFAD2-2, indicating that the differences in functional expression are likely to be associated with their sequence variation, transmembrane topology characteristic, as well as protein structure exposed in ER. Although they exhibited low variation (9 %) from one another, membrane topology prediction indicated that they are highly hydrophobic and contain five and six transmembrane domains, respectively. Moreover, dissimilar topological orientation in ER membrane regarding histidine box, and N- and C-terminus localization was observed. It has been investigated that the three conserved histidine-enriched clusters coordinate diiron atoms at the active site center, which affects the enzyme catalytic efficiency. The N- and C-terminal regions also influence protein stability [3, 39]. Hence, the functional differences can be strongly suggested by the diversity of these desaturase genes. Furthermore, posttranscriptional events such as mRNA stability, translational efficiency, enzyme half-life, or enzyme catalytic efficiency are proposed to result in PpFAD2 function and might be helpful for investigation in further research. It has been documented that plant FADs are also short-lived proteins whose abundance can be modulated to regulate the amount of PUFAs produced [3]. Cultivation of soybean FAD2-transformed yeast cells at cooler growth temperature further increased FAD2 protein half-life and corresponding steady-state amount of protein, resulting in an increase in LA content [44].

To date, certain families of methyl-end desaturases from various organisms have been investigated, covering both mono- and bifunctional desaturase activities. In our study,

a yeast feeding experiment supplied with LA (18:2 $\Delta^{9,12}$) in the culture medium did not illustrate any fatty acid production in the transformed yeast cells (Table 2). This confirms that both PpFAD2 polypeptides are monofunctional Δ^{12} -fatty acid desaturases, not linoleate Δ^{15} -desaturases. In contrast, the bifunctional Δ^{12}/Δ^{15} -fatty acid desaturases from the protozoa *A. castellanii* and the fungus *Coprinus cinereus* have been documented to convert C16:1 Δ^9 and C18:1 Δ^9 fatty acid substrates to either 16:2 $\Delta^{9,12}$ and 18:2 $\Delta^{9,12}$, or 16:3 $\Delta^{9,12,15}$ and 18:3 $\Delta^{9,12,15}$ [37, 52].

Yeast cells are eukaryotic and contain an ER that is necessary for the activity of plant FAD2 enzymes that are integral membrane proteins. In addition, yeast cells lack a FAD2-type gene, and they normally do not synthesize LA (C18:2). Hence, yeast expression systems are commonly employed for functional identification of eukaryotic fatty acid desaturases in the ER, such as *O. europaea*, *R. arrhizus* Δ^{12} -desaturases [10, 49], *P. patens* Δ^5 -, Δ^6 -desaturases [9, 17], and *P. patens* Δ^6/Δ^9 - and $\Delta^5/\Delta^6/\Delta^9$ -elongases [4]. In this study, functional identification of PpFAD2s by heterologous expression in *S. cerevisiae* was also performed. Nevertheless, the obtained LA synthesis from the endogenous OA of *S. cerevisiae* by additionally introducing PpFAD2s was relatively low compared with the high LA amount produced from intact *P. patens*. This indicates that the expression system is the key issue affecting enzyme expression. Although the heterologous expression system in yeast is normally used to study the function of plant PUFA biosynthesis enzymes, numerous factors still mediate the enzyme activity, such as yeast strain, promoter type, and culture condition [4, 10, 35]. In our experiments, the influence of a physical parameter was then examined. Obviously, the accumulation of hexadecadienoic acid (16:2 $\Delta^{9,12}$) and LA (18:2 $\Delta^{9,12}$) in transformed yeasts was further increased by lowering the culture temperature (to 15 °C). The elevated level of unsaturated fatty acids in yeasts at low temperature was strongly associated with the activity of the desaturase, which is a temperature-sensitive enzyme [15, 33, 36]. This might also be attributable to the desaturase genes receiving signals from a specific sensor in the cytoplasmic membrane [47]. An increase in unsaturated fatty acid products at low temperature might be a response to maintain membrane fluidity and function, allowing yeasts to acclimatize to low-temperature stress. This is also in agreement with the role of a microsomal oleate desaturase in sunflower (*H. annuus*) seeds, which at a low temperature (10 or 20 °C) brought about an increase in the FAD2 activity, whereas culture at a higher temperature (30 °C) resulted in a lower level of activity [23, 36].

Even though we found that the two FAD2s from *P. patens* demonstrated only 9 % sequence deviation, we verified that both carried out different potential

Δ^{12} -desaturation activities with regard to 16:1 Δ^9 and C18:1 Δ^9 . PpFAD2-1 not only contributed greater desaturation activity but also was much more responsive to temperature change than PpFAD2-2. The higher thermal stability of PpFAD2-2 is probably due to the C-terminal aromatic retrieval motif, which is not present in PpFAD2-1. The presence of polar amino acids including asparagines (N) and glutamine (Q) was observed in the C-terminus of PpFAD2-2, while PpFAD2-1 contained basic dilysine (K) residue. The amide functional group of asparagine (N) and glutamine (Q) is highly polar and can participate in multiple hydrogen-bond interactions. They can therefore fulfill an important role in stabilizing local folded structure in proteins [46]. Moreover, Southern blotting clearly confirmed the different genetic information present in PpFAD2-1 and PpFAD2-2, with only a single copy within the *P. patens* genome. Similarly, a single copy of FAD2 was documented in *T. majus* [26], whereas at least two copies of each OeFAD2 gene were observed in the olive genome [10]. Since we discovered two FAD2s in *P. patens* showing a degree of difference in their Δ^{12} -desaturase activity and thermal responsiveness, this might suggest that *P. patens* requires both for maintenance of growth and fatty acid restoration. In addition, it has been demonstrated that the diverse expression levels of two olive microsomal oleate desaturase (FAD2) transcripts depended on developing tissues [10]. This effect may also possibly participate in the expression level of PpFADs. Our finding therefore provides evidence for further characterization of whether they are tissue or developmentally regulated.

In summary, we have cloned and identified the function of two microsomal Δ^{12} -desaturases (PpFAD2s) from *P. patens* that are involved in synthesis of an essential fatty acid, LA. Our analysis also provides clearer understanding of the accumulation of the main fatty acid precursor, LA, which is necessary for production of further LC-PUFAs and improves knowledge of the PUFA biosynthesis pathway in *P. patens*. Future studies on gene inactivation are still required to determine the in vivo functions of the genes or fatty acids. However, this finding may ultimately permit predictable manipulation of the PUFA composition of plant membrane to improve the vigor and viability of crop plants.

Acknowledgments This research was supported by Prince of Songkla University (PSU, PHA540648S), the Higher Education Research Promotion and National Research University Project of Thailand, Office of the Higher Education Commission (PHA5405395), and the Marine Natural Products Research Unit (MNP) at the Faculty of Pharmaceutical Sciences, PSU. We gratefully acknowledge Assist. Prof. Dr. Akkharawit Kanjana-Opas for providing the laboratory facilities and also thank Dr. Brian Hodgson of PSU for assistance with the English.

References

- Ashton NW, Cove DC (1977) The isolation and preliminary characterization of auxotrophic and analogue resistance mutants in the moss *Physcomitrella patens*. *Mol Gen Genet* 154:87–95
- Avelange-Macherel MH, Macherel D, Wada H, Murata N (1995) Site-directed mutagenesis of histidine residues in the Δ^{12} acyl-lipid desaturase of *Synechocystis*. *FEBS Lett* 361:111–114
- Dyer JM, Mullen RT (2008) Engineering plant oils as high-value industrial feedstocks for biorefining: the need for underpinning cell biology research. *Physiol Plantarum* 132:11–32
- Eiamsa-ard P, Kanjana-Opas A, Cahoon EB, Chodok P, Kaewsuwan S (2013) Two novel *Physcomitrella patens* fatty acid elongases (ELOs): identification and functional characterization. *Appl Microbiol Biotechnol* 97:3485–3497
- Falcone DL, Gibson SG, Lemieux B, Somerville C (1994) Identification of a gene complements an *Arabidopsis* mutant deficient in chloroplast $\omega 6$ desaturase activity. *Plant Physiol* 106:1453–1459
- Freeman MP, Hibbeln JR, Wisner KL, Davis JM, Mischoulon D, Peet M, Keck PE, Marangell LB, Richardson AJ, Lake J, Stoll AL (2006) Omega-3 fatty acids: evidence basis for treatment and future research in psychiatry. *J Clin Psychiatry* 67:1954–1967
- Garcia-Maroto F, Garrido-Cardenas JA, Michaelson LV, Napier JA, Alonso DL (2006) Cloning and molecular characterisation of a $\Delta 8$ -sphingolipid-desaturase from *Nicotiana tabacum* closely related to $\Delta 6$ -acyl-desaturases. *Plant Mol Biol* 64:241–250
- Gill I, Valivety R (1997) Polyunsaturated fatty acids, part 1: occurrence, biological activities and application. *Tibtech* 15: 401–409
- Girke T, Schmidt H, Zahringer U, Reski R, Heinz E (1998) Identification of a novel $\Delta 6$ -acyl-group desaturase by targeted gene disruption in *Physcomitrella patens*. *Plant J* 15:39–48
- Hernandez ML, Mancha M, Martinez-Rivas JM (2005) Molecular cloning and characterization of genes encoding two microsomal oleate desaturases (FAD2) from olive. *Phytochemistry* 66:1417–1426
- Hitz WD, Carlson TJ, Booth JR Jr, Kinney AJ, Stecca KL, Yadav NS (1994) Cloning of a higher-plant plastid $\omega 6$ fatty acid desaturase cDNA and its expression in a cyanobacterium. *Plant Physiol* 105:635–641
- Horrobin DF (1992) Nutritional and medical importance of gamma-linolenic acid. *Prog Lipid Res* 31:163–194
- Huang YS, Chaudhary S, Thurmond JM, Bobik EG Jr, Yuan L, Chan GM, Kirchner SJ, Mukerji P, Knutson DS (1999) Cloning of $\Delta 12$ - and $\Delta 6$ -desaturases from *Mortierella alpina* and recombinant production of γ -linolenic acid in *Saccharomyces cerevisiae*. *Lipids* 34:649–659
- Jackson MR, Nilsson T, Peterson PA (1990) Identification of a consensus motif for retention of transmembrane proteins in the endoplasmic reticulum. *EMBO J* 9:3153–3162
- Jiang H, Gao K (2004) Effects of lowering temperature during culture on the production of polyunsaturated fatty acids in the marine diatom *Phaeodactylum tricornutum* (Bacillariophyceae). *J Phycol* 40:651–654
- Kaewsuwan S, Bunyapraphatsara N, Cove DJ, Quatrano RS, Chodok P (2010) High level production of adrenic acid in *Physcomitrella patens* using the algae *Pavlova* sp. Δ^5 -elongase gene. *Bioresour Technol* 101:4081–4088
- Kaewsuwan S, Cahoon EB, Perroud PF, Wiwat C, Panvisavas N, Quatrano RS, Cove DJ, Bunyapraphatsara N (2006) Identification and functional characterization of the moss *Physcomitrella patens* Δ^5 -desaturase gene involved in arachidonic and eicosapentaenoic acid biosynthesis. *J Biol Chem* 281:21988–21997

18. Kang J, Snapp AR, Lu C (2011) Identification of three genes encoding microsomal oleate desaturases (FAD2) from the oil seed crop *Camelina sativa*. *Plant Physiol Biochem* 49:223–229
19. Knight CD, Cove DJ, Cuming AC, Quatrano RS (2002) Moss gene technology. In: Gilmartin PM, Bowter C (eds) *Molecular plant biology*. Oxford University Press, NY, pp 285–302
20. Krasowska A, Dziadkowiec D, Polinceusz A, Plonka A, Lukaszewicz M (2007) Cloning of flax oleic fatty acid desaturase and its expression in yeast. *J Am Oil Chem Soc* 84:809–816
21. Li L, Wang X, Gai J, Yu D (2007) Molecular cloning and characterization of a novel microsomal oleate desaturase gene from soybean. *J Plant Physiol* 164:1516–1526
22. Los DA, Murata N (1998) Structure and expression of fatty acid desaturase. *Biochim Biophys Acta* 1394:3–15
23. Martinez-Rivas JM, Garcoa-Diaz MT, Mancha M (2000) Temperature and oxygen regulation of microsomal desaturase (FAD2) from sunflower. *Biochem Soc Trans* 28:890–892
24. Martinez-Rivas JM, Sperling P, Luehs W, Heinz E (2001) Spatial and temporal regulation of three different microsomal oleate desaturase genes (FAD2) from normal-type and high-oleic varieties of sunflower (*Helianthus annuus* L.). *Mol Breed* 8:159–168
25. McCartney AW, Dyer JM, Dhanoa PK, Kim PK, Andrews DW, McNew JA, Mullen RT (2004) Membrane-bound fatty acid desaturases are inserted co-translationally into the ER and contain different ER retrieval motifs at their carboxy termini. *Plant J* 37:156–173
26. Mietkiewska E, Brost JM, Giblin EM, Francis T, Wang S, Reed D, Truksa M, Taylor DC (2006) A *Tropaeolum majus* FAD2 cDNA complements the fad2 mutation in, transgenic *Arabidopsis* plants. *Plant Sci* 171:187–193
27. Miquel MF, Browse JA (1994) High-oleate oilseeds fail to develop at low temperature. *Plant Physiol* 106:421–427
28. Ohlrogge J, Browse J (1995) Lipid biosynthesis. *Plant Cell* 7:957–970
29. Passorn S, Laoteng K, Rachadawong S, Tanticharoen M, Cheevadhanarak S (1999) Heterologous expression of *Mucor rouxii* Δ^{12} -desaturase gene in *Saccharomyces cerevisiae*. *Biochem Biophys Res Commun* 263:47–51
30. Pereira SL, Leonard AE, Mukeri P (2003) Recent advances in the study of fatty acid desaturases from animals and lower eukaryotes. *Prostaglandins Leukot Essent* 68:97–106
31. Peyou-Ndi MM, Watts JL, Browse J (2000) Identification and characterization of an animal Δ^{12} fatty acid desaturase gene by heterologous expression in *Saccharomyces cerevisiae*. *Arch Biochem Biophys* 376:399–408
32. Pirtle IL, Kongcharoensuntorn W, Nampaisansuk M, Chapman KD, Pirtle RM (2001) Molecular cloning and functional expression of the gene for a cotton Δ^{12} -fatty acid desaturase (FAD2). *Biochim Biophys Acta* 1522:122–129
33. Sakamoto T, Higshi S, Wada H, Murata N, Brayand DA (1994) Low-temperature-induced desaturation of fatty acids and expression of desaturase genes in the cyanobacterium *Synechococcus* sp. PCC 7002. *Plant Mol Biol* 26:249–263
34. Sakamoto T, Wada H, Nishida M, Ohmori M, Murata N (1994) Identification of conserved domains in the Δ^{12} desaturases of cyanobacteria. *Plant Mol Biol* 24:643–650
35. Sanchez-Garcia A, Mancha M, Heinz E, Martinez-Rivas JM (2004) Differential temperature regulation of three sunflower microsomal oleate desaturase (FAD2) isoforms overexpressed in *Saccharomyces cerevisiae*. *Eur J Lipid Sci Technol* 106:583–590
36. Samiento C, Garces R, Mancha M (1998) Oleate destauration and acyl turnover in sunflower (*Helianthus annuus* L.) seed lipids during rapid temperature adaptation. *Planta* 205:595–600
37. Sayanova O, Haslam R, Guschina I, Lloyd D, Christie WW, Harwood JL, Napier JA (2006) A bifunctional Δ^{12} , Δ^{15} -desaturase from *Acanthamoeba castellanii* directs the synthesis of highly unusual *n*-1 series unsaturated fatty acids. *J Biol Chem* 281:36533–36541
38. Sayanova OV, Napier JA (2004) Eicosapentaenoic acid; biosynthetic routes and the potential for synthesis in transgenic plants. *Phytochemistry* 65:147–158
39. Shanklin J, Cahoon EB (1998) Desaturation and related modifications of fatty acids. *Annu Rev Plant Physiol Plant Mol Biol* 49:611–641
40. Shanklin J, Achim C, Schmidt H, Fox BG, Munck E (1997) Mossbauer studies of alkane-hydroxylase: evidence for a diiron cluster in an integral membrane enzyme. *Proc Natl Acad Sci USA* 94:2981–2986
41. Shanklin J, Whittle E, Fox BG (1994) Eight histidine residues are catalytically essential in a membrane-associated iron enzyme, stearoyl-CoA desaturase, and are conserved in alkane hydroxylase and xylene monooxygenase. *Biochemistry* 33:12787–12794
42. Simopoulos AP (2002) Omega-3 fatty acids in inflammation and autoimmune disease. *J Am Coll Nutr* 21:495–505
43. Sperling P, Libisch B, Zahringer U, Napier JA, Heinz E (2001) Functional identification of a Δ^8 -sphingolipid desaturase from *Borago officinalis*. *Arch Biochem Biophys* 388:293–298
44. Tang GQ, Novitzky WP, Carol Griffin H, Huber SC, Dewey RE (2005) Oleate desaturase enzymes of soybean: evidence of regulation through differential stability and phosphorylation. *Plant J* 44:433–446
45. Ueshima H, Stamler J, Elliott P, Brown JJ, Carnethon MR, Daviglus ML, He K, Moag-Stahlberg A, Rodriguez BL, Steffen LM, VanHom L, Yarnell J, Zhou B (2007) Food omega-3 fatty acid intake of individuals (total, linolenic acid, long-chain) and their blood pressure INTERMAP study. *Hypertension* 50:313–319
46. Vasudev PG, Banerjee M, Ramakrishnan C, Balaram P (2012) Asparagine and glutamine differ in their propensities to form specific side chain-backbone hydrogen bonded motifs in proteins. *Proteins* 80:991–1002
47. Vigh L, Los DA, Horvath I, Murata N (1993) The primary signal in the biological perception of temperature: pd-catalyzed hydrogenation of membrane lipids stimulated the expression of the desA gene in *Synechocystis* PCC6803. *Proc Natl Acad Sci USA* 90:9090–9094
48. Von Schacky C (2006) A review of omega-3 ethyl esters for cardiovascular prevention and treatment of increased blood triglyceride levels. *Vasc Health Risk Manag* 2:251–262
49. Wei D, Li M, Zhang X, Ren Y, Xing L (2004) Identification and characterization of a novel Δ^{12} -fatty acid desaturase gene from *Rhizopus arrhizus*. *FEBS Lett* 573:45–50
50. Zank TK, Zahringer U, Beckmann C, Pohnert G, Boland W, Holtorf H, Reski R, Lerchl J, Heinz E (2002) Cloning and functional characterisation of an enzyme involved in the elongation of Δ^6 -polyunsaturated fatty acids from the moss *Physcomitrella patens*. *Plant J* 31:255–268
51. Zhang JT, Zhu JQ, Zhum Q, Liu H, Gao XS, Zhang HX (2009) Fatty acid desaturase-6 (Fad6) is required for salt tolerance in *Arabidopsis thaliana*. *Biochem Biophys Res Commun* 390:469–474
52. Zhang S, Sakuradani E, Ito K, Shimizu S (2007) Identification of a novel bifunctional Δ^{12}/Δ^{15} fatty acid desaturase from a basidiomycete, *Coprinus cinereus* TD#822-2. *FEBS Lett* 581:315–319
53. Zhou XR, Horne I, Damcevski K, Haritos V, Green A, Singh S (2008) Isolation and functional characterization of two independently-evolved fatty acid Δ^{12} -desaturase genes from insects. *Insect Mol Biol* 17:667–676